



HAL
open science

Microgrid Frequency Stability: A Proactive Scheme Based on Dynamic Predictions

Gian Paramo, Arturo Bretas, Sean Meyn

► **To cite this version:**

Gian Paramo, Arturo Bretas, Sean Meyn. Microgrid Frequency Stability: A Proactive Scheme Based on Dynamic Predictions. 2024 Conference on Innovative Smart Grid Technologies, North America (ISGT NA 2024), IEEE, Feb 2024, Washington, United States. hal-04471094

HAL Id: hal-04471094

<https://hal.science/hal-04471094>

Submitted on 21 Feb 2024

HAL is a multi-disciplinary open access archive for the deposit and dissemination of scientific research documents, whether they are published or not. The documents may come from teaching and research institutions in France or abroad, or from public or private research centers.

L'archive ouverte pluridisciplinaire **HAL**, est destinée au dépôt et à la diffusion de documents scientifiques de niveau recherche, publiés ou non, émanant des établissements d'enseignement et de recherche français ou étrangers, des laboratoires publics ou privés.

Copyright

Microgrid Frequency Stability: A Proactive Scheme Based on Dynamic Predictions

Gian Paramo * Arturo Bretas †‡ Sean Meyn *

* Department of Electrical and Computer Engineering, University of Florida, Gainesville, FL

† G2Elab, Grenoble INP, CNRS, Université Grenoble Alpes, 38000 Grenoble, France

‡ Distributed Systems Group, Pacific Northwest National Laboratory, 99354 Richland, USA

gianparamo@ufl.edu, arturo.suman-bretas@cnrs.fr, meyn@ece.ufl.edu

Abstract—The dynamic nature of microgrids introduces challenges in the context of frequency stability. This work presents a framework where the future state of microgrid frequency is predicted and corrective actions are optimized. Predictions are generated through Bayesian filters leveraging synchronized data acquired via PMUs. Taking a proactive approach makes it possible to optimize corrective actions considering dynamic system conditions. Testing is conducted via Matlab simulations. The performance of the solution presented in this work is compared to traditional load-shedding schemes and to predictive solutions found in literature. The results indicate that the proposed framework outperforms both. Some of the advantages of this framework include a reduction in amount of load dropped during compensation, the use of adaptive parameters which eliminates the need to simulate contingency conditions, and dynamic uncertainty quantification provided the particle filter.

Index Terms—Phasor Measurement Units, Power System Protection, Underfrequency Load Shedding, Particle Filters.

I. INTRODUCTION AND LITERATURE REVIEW

The flexibility and dynamic nature of microgrids pose challenges in terms of protection and control. Creating a protection scheme that can cover the many and rapidly changing operating conditions often observed in these systems is difficult [1]. Another important, yet unresolved, issue effecting the operation and reliability of microgrids is the need to find generation-load balance after an island is formed [2]. The process of attaining generation-load balance for a microgrid during islanded operation is fundamentally the same as finding generation-load balance in the macrogrid: Sources with available capacity are actuated and excess load is dropped [2]. The limitations of state-of-the-art frequency stability schemes are also the same at both, the micro and the macro level. Currently, the majority of automatic underfrequency load shedding (UFLS) solutions are built on decentralized architectures with little to no feedback, and operate at the feeder level [3]. Traditional UFLS schemes are reactive in the context that corrective actions are taken only after the system has entered a critical state. This leads to two commonly observed issues: delayed response and overshedding [4].

In order to overcome some of these challenges, the solution presented in [5] utilizes an adaptive algorithm based on power

measurements to drive a load-shedding process. In [6], a mixed integer linear programming (MILP) algorithm is used to optimize a cost function after a drop in frequency is detected via the rate of change of frequency (RoCoF). An adaptive, multi-stage load shedding controller is presented in [7], where local voltage and frequency measurements are used to identify locations where compensation is required. In [8], a fuzzy logic control algorithm is used to drive the virtual inertia in a microgrid in response to changes in power injections and system frequency oscillations. A cooperative control approach of neighboring distributed energy resources (DERs) is introduced in [9]. In [10], neural networks are used to optimize the response of a cooperative control scheme for microgrid stability.

Predictive schemes in power systems have been suggested in various forms. A model predictive control approach is developed in [11] to optimize microgrid operation. In [12], measurements are collected via Phasor Measurement Units (PMUs). Data is processed as a time series, and short term predictions are made. The work presented in [13] predicts post disturbance steady state frequency. Active power injections of synchronous condensers are used by [14] to detect load-generation imbalances proactively. Meanwhile [15], develops a method where PMU measurements and polynomial curve-fitting are used to make predictions.

In [16], frequency control is carried out by actuating fast acting DERs through an algorithm based on the Extended Kalman filter. In [17], a predictive stability scheme was presented where the center of oscillations and the total energy of the system are used to detect unstable conditions shortly before the system enters a critical condition.

Solutions found in literature have the following limitations in common: Most cannot be supported by existing technology. For instance, these approaches normally rely on PMU measurements with high reporting rates (in some cases over 100 frames per second). This work, by contrast, is based on PMU reporting rates of 30 frames per second, as this rate would place a lighter burden on communication infrastructures [18]–[20].

Second, the techniques surveyed above fall into one of two categories: Data driven solutions and physics-based solutions. This work proposes a hybrid approach where data complements physics-based models. This enables the solution

This work was partially funded by the U.S. Department of Energy under Contract DE-AC05-76RL01830.

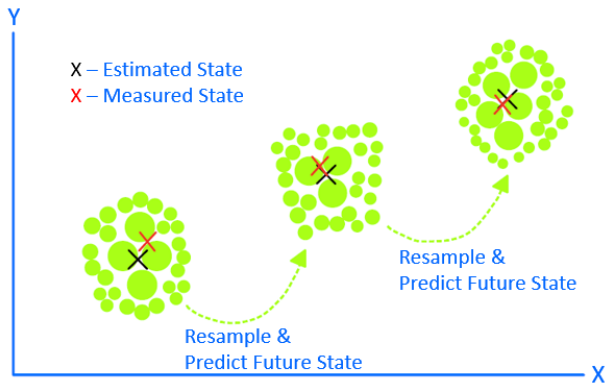


Fig. 1: Particle Based Sampling.

to produce results that take into account system dynamics and the physical limits of the system. The end product is a proactive framework for automatic frequency stability where model uncertainty is continuously updated [21].

The main contribution of this work lies in the application of the PF in the area of microgrid stability. The PF is leveraged to produce a hybrid solution that integrates a data-driven approach with physics-based equations.

The rest of the paper is structured as follows: Section II provides an overview of the technique, including an introduction to the particle filter. The complete scheme is summarized in Section III. Case studies and results can be found in Section IV. Concluding remarks are given in Section V.

II. DYNAMIC PREDICTIONS

A. Particle Filter

The particle filter (PF) is an approach to state estimation that combines Bayesian inference with the Monte Carlo method. The premise behind this type of estimation is that, *it is easier to approximate a probability distribution, than it is to approximate an arbitrary nonlinear function or transformation* [22]. Two advantages of the PF compared to other filtering techniques are that the PF is not limited to Gaussian distributions. The PF also offers inherent uncertainty quantification [23]. The PF estimates an underlying probability distribution via samples called particles. Using a simple object tracking problem as an example, the process can be summarized as follows: First, a set of particles are placed around the predicted location of the object. Then measurements are used to assign weights to the particles. Particles closer to the measurements are given a higher weight. The object's location can be estimated by calculating the weighted average of the particles. The cluster of particles is then updated in two ways: First, particles with lower weights are redistributed around particles with higher weights. Then, the cluster itself is moved in accordance with the measurements and a system model. The process is then repeated at each time step. This is illustrated in fig.1.

The problem of tracking the frequency of a power system is somewhat similar to tracking a particle moving cross a 2-D plane. For frequency tracking, the x-axis corresponds to time,

while the y-axis corresponds to the frequency value at that particular moment. A sinusoidal function and the change in frequency, in this case Δy , are part of the system model in this work. A complete derivation of the PF is omitted due to space constraints, but it can be found as part of the tutorial presented in [21]. For the interested reader, a comparison among several types of Bayesian filters can be found in [24].

B. Prediction

RoCoF is used as the primary means of disturbance detection. RoCoF offers a reasonable balance between adaptability and ease of implementation. After a disturbance is identified via the RoCoF, a prediction is made by feeding Artificial Data Points (ADPs) to the PF. ADPs are used to extend the horizon of the predictions produced by the PF beyond the typical $k+1$ time steps. This is an iterative process that creates a vector that is then used by the filter to make predictions:

$$ADP_i = ADP_{i-1} + t_s f' + t_s^2 f'' \quad (1)$$

ADP_{i-1} refers to the previous ADP. The average first derivative of frequency is represented by f' , while the average second derivative of frequency is represented by f'' . Finally, t_s represents the time window of the derivatives [23], [25].

C. Load Excess Calculation

Following a prediction, a load excess factor is calculated using a formula derived from the swing equation [3]:

$$L = \frac{R_p H (1 - \frac{f_p^2}{f_1^2})}{p(f_p - f_1)} \quad (2)$$

In which L represents the load excess factor, H is the inertia coefficient, p represents the power factor, and R_p is the predicted rate of change of frequency.

$$R_p = \frac{f_p - f_1}{t_s} \quad (3)$$

During a prediction, R_p is calculated as the difference between the current frequency measurement f_1 , and the predicted frequency measurement f_p , divided by the time window t_s . In this work, the state of frequency is predicted one second into the future.

III. SCHEME OVERVIEW

A. Distributed Operation

This work takes a distributed approach where areas (islands) are established based on PMU observability, as well as generation capacity. There is cooperation between neighboring areas, as PMUs near the edge of one area share information with adjacent areas.

PMUs are assumed to have a reporting rate of 30 measurements per second. Similar techniques in literature assume delays of roughly 0.5 seconds or less [13], [15]. This delay accounts for communication latency and delays related to equipment operation, such as breaker trip times. This work makes the same assumption regarding the delay of the response. The local

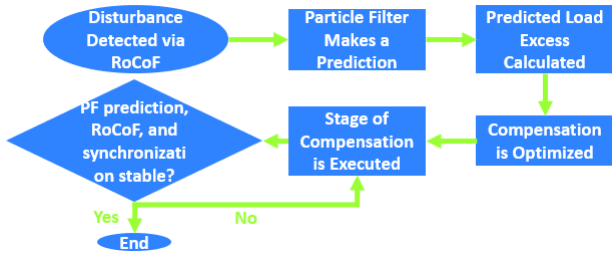


Fig. 2: Process flow.

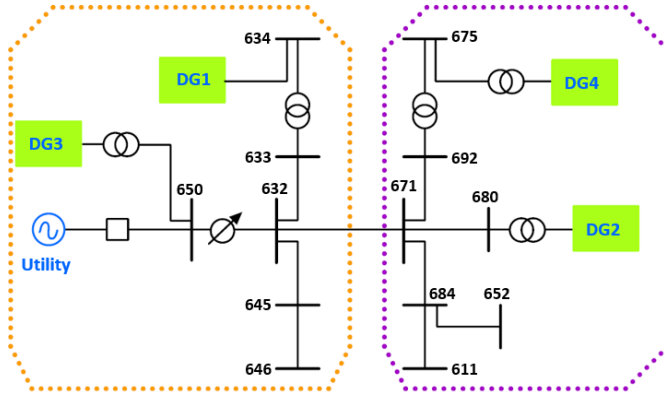


Fig. 3: One Line Diagram of the Test System.

inertia of each area is computed online as presented in [26]. This value is then used to calculate the load excess factor via equation 2.

B. Optimized Response

A MILP algorithm is used to optimize the response after a disturbance. Three sources of compensation are considered in this work, these include: The actuation of DERs, shedding of non-critical loads (residential customers), and shedding of sensitive loads (industrial customers). Each one of them carries a different penalty for use, with DERs having the lowest penalty, and sensitive loads carrying the highest. The loading and capacity of the sources of compensation are updated in real time. This information is already captured by most utilities. After a suitable combination of compensation agents has been identified, trip commands are sent to the selected breakers. The process flow, including critical steps are presented in fig. 2.

IV. CASE STUDY

The case study presented in this section is based on a modified version of the IEEE-13 Bus test system used in [27]. The dynamics are modeled in *Simulink*, while the analytics and predictions are performed in *Matlab*. A One-Line diagram of the system is provided in fig. 3. System parameters, and per-phase loading information can be found in tables 1 and 2 of [27]. Gaussian noise was added to the PMU measurements. It must be noted that the PF performs better when there is a moderate amount of noise in the measurements. This is

because noise is related to how particles are distributed during the predict and update steps [24]. To account for processing and communication delays, corrective actions are taken half a second after each prediction is made.

A. Case Study: Sub-islanding is Prevented

Initial conditions are as follows: All sources, including utility and DGs are online. The utility breaker opens at 1 second, creating an island with four DGs and a load excess of around 20%. Due to topology and physical distances, this larger island can be broken into two smaller islands as depicted in fig. 3. The scheme will attempt to keep smaller islands from being formed by keeping the DGs synchronized until frequency is stabilized. DG rotor angles will be tracked during this case study. Fig. 4 depicts the complete response of the system when the PF-based scheme is used to mitigate these disturbances.

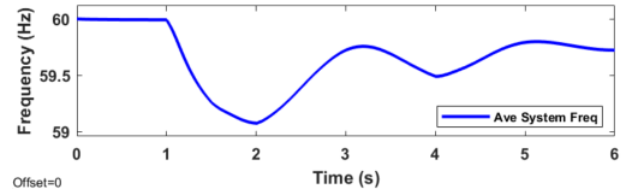


Fig. 4: Frequency Response with PF Mitigation.

The prediction and mitigation process is as follows: An initial prediction is made after RoCoF thresholds are surpassed. This is illustrated in fig. 5.

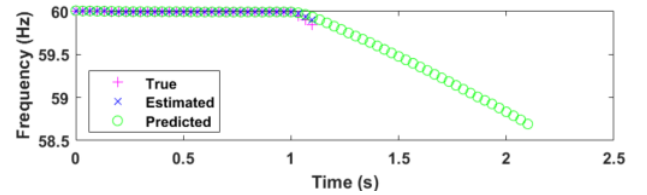


Fig. 5: Initial PF Prediction.

Half a second after the prediction is made (to account for communication and equipment delays), the first stage of compensation is carried out. Immediately after this stage of compensation is completed, a new prediction is made. This is shown in fig. 6.

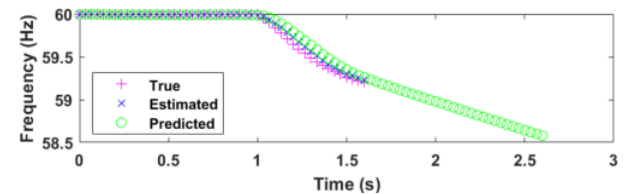


Fig. 6: Second PF Prediction.

Since this new prediction shows that frequency is still on the decline, a new stage of compensation and prediction is carried out at around 2 seconds. This is illustrated in fig. 7.

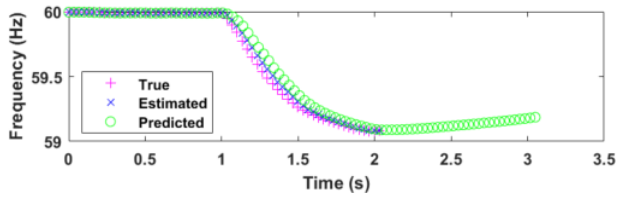


Fig. 7: Third PF Prediction.

This time however, the prediction shows the system’s frequency climbing back to normal ranges. A subsequent stage of compensation is put on hold until the a new decline in frequency is detected at roughly 3.5 seconds, as shown in fig. 8.

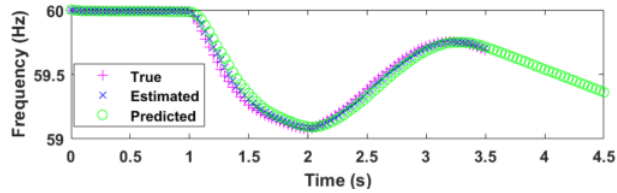


Fig. 8: Fourth PF Prediction.

Based on this prediction a new stage of compensation is carried out at 4 seconds. Immediately after, a new prediction is made, this is shown in fig. 9.

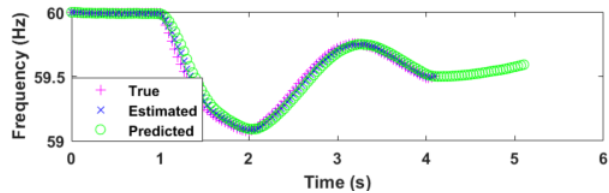


Fig. 9: Final PF Prediction.

With frequency returning to normal ranges, the compensation algorithm stops. The complete response is shown in fig. 4, while difference in rotor angles is shown in fig. 10. The proposed scheme was able to stabilize the system while keeping all four DGs synchronized.

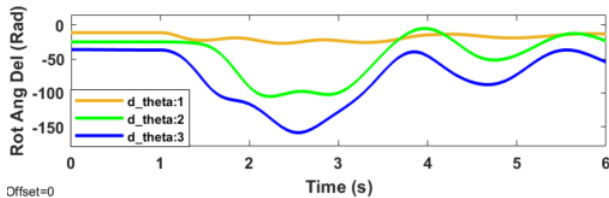


Fig. 10: Rotor Angles with PF-based Mitigation.

In fig. 10, d-theta values are the rotor angle differences between DG1 and the other three machines.

B. Traditional UFLS Performance

A traditional UFLS scheme is used to mitigate the same disturbances. Fixed settings are used, and the complete response is shown in fig. 11.

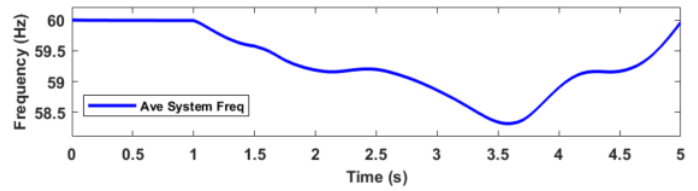


Fig. 11: Frequency Response with Traditional UFLS Scheme.

In this case the traditional UFLS scheme was able to stabilize frequency, however, synchronization between the DGs is lost as illustrated in fig. 12.

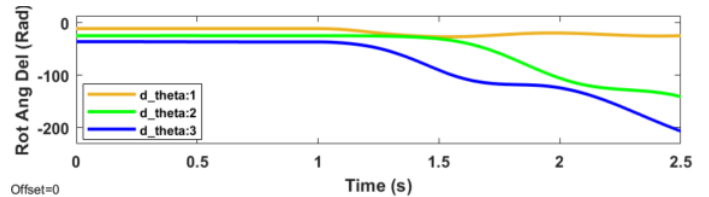


Fig. 12: Rotor Angles with Traditional UFLS Mitigation.

In addition to maintaining synchronization between the islands, the solution presented in this paper produced corrective actions that are optimized taking into account dynamic system conditions. The traditional UFLS scheme on the other hand, simply drops load indiscriminately as frequency thresholds are surpassed [28]. In this work it was assumed that there was enough load available for shedding for the traditional UFLS scheme to stabilize the system.

C. Polynomial Curve Fitting

Finally, the framework presented in [15] is used to mitigate the same disturbances. In [15], predictions are produced via Polynomial Curve-Fitting (PCF). The limitations of the PCF-based solution become clear at the 2 second mark in fig. 13, and once again at the 4 second mark in fig. 14.

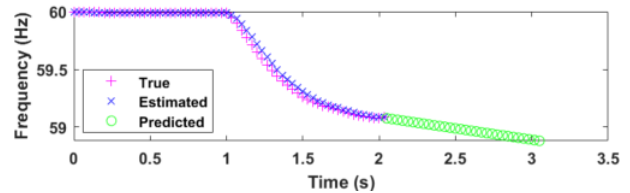


Fig. 13: PCF-based Prediction.

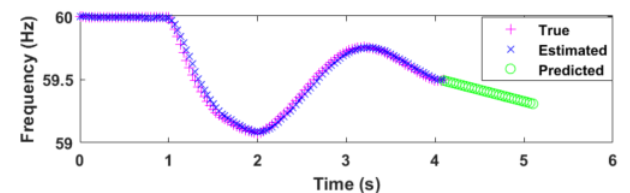


Fig. 14: PCF-based Prediction.

The PCF-based solution is unable to leverage the dynamics of the system the way the PF-based solution can. As a result of this, in both cases, the PCF-based solution predicts that frequency will continue to decline and the scheme will

continue to compensate, leading to an unnecessary loss of customers. By contrast, as shown in fig. 7 and in fig. 9, the PF-based scheme is able to make predictions that decrease the amount of compensation utilized. In simulation based testing the method presented in this paper was able to stabilize the system while shedding 25% to 50% less load than the PCF-based technique. These results are consistent with the results obtained in [23].

V. CONCLUSION

A proactive frequency stability framework for microgrids was presented in this work. After a disturbance was detected the future state of frequency was predicted via particle filters. Being able to predict a critical state a few seconds in advance made it possible to optimize corrective actions. During testing this solution outperformed UFLS schemes, as well as frameworks found in literature by reducing the amount of load shed in response to disturbances. Future work will focus on validation on larger and more complex systems.

REFERENCES

- [1] A. Hooshyar, and R. Iravani, "Microgrid Protection," in Proceedings of the IEEE, vol. 105, no. 7, pp. 1332-1353, July 2017, doi: 10.1109/JPROC.2017.2669342.
- [2] M. Farrokhbadi et al., "Microgrid Stability Definitions, Analysis, and Examples," in IEEE Transactions on Power Systems, vol. 35, no. 1, pp. 13-29, Jan. 2020, doi: 10.1109/TPWRS.2019.2925703.
- [3] S. H. Horowitz, and A. G. Phadke, *Power System Relaying*, 4th, Wiley, West Sussex, United Kingdom, 2014.
- [4] L. Sigrist, L. Rouco, and F. M. Echavarren, "A review of the state of the art of UFLS schemes for isolated power systems," in International Journal of Electrical Power & Energy Systems, vol 99, pp. 525-539, 2018, doi: 10.1016/j.ijepes.2018.01.052.
- [5] V. Mynam, and A. Guzmán, "Islanding Detection and Adaptive Load Shedding," SEL Application Note (AN2009-59), September 2009.
- [6] M. Javadi, Y. Gong, and C. Y. Chung, "Frequency Stability Constrained Microgrid Scheduling Considering Seamless Islanding," in IEEE Transactions on Power Systems, vol. 37, no. 1, pp. 306-316, Jan. 2022, doi: 10.1109/TPWRS.2021.3086844.
- [7] M. Marzband, M.M. Moghaddam, M.F. Akorede, and G. Khomeyran, "Adaptive load shedding scheme for frequency stability enhancement in microgrids," in Electric Power Systems Research, vol. 22, no. 5, pp. 78-86, Nov. 2016, doi: 10.1016/j.epsr.2016.06.037.
- [8] T. Kerdphol, M. Watanabe, K. Hongesombut, and Y. Mitani, "Self-Adaptive Virtual Inertia Control-Based Fuzzy Logic to Improve Frequency Stability of Microgrid With High Renewable Penetration," in IEEE Access, vol. 7, pp. 76071-76083, 2019, doi: 10.1109/ACCESS.2019.2920886.
- [9] R. D. Trevizan, M. Ayar, A. S. Bretas, and S. Obuz, "Cooperative Control of Energy Storage for Transient Stability Enhancement," 2018 IEEE Power & Energy Society General Meeting (PESGM), Portland, OR, USA, 2018, pp. 1-5, doi: 10.1109/PESGM.2018.8586028.
- [10] W. Gu, W. Liu, Z. Wu, B. Zhao, and W. Chen, "Cooperative Control to Enhance the Frequency Stability of Islanded Microgrids with DFIG-SMES," Energies, vol. 6, no. 8, pp. 3951-3971, Aug. 2013, doi: 10.3390/en6083951.
- [11] A. Parisio, E. Rikos, and L. Glielmo, "A Model Predictive Control Approach to Microgrid Operation Optimization," in IEEE Transactions on Control Systems Technology, vol. 22, no. 5, pp. 1813-1827, Sept. 2014, doi: 10.1109/TCST.2013.2295737.
- [12] N. G. Bretas, and A. G. Phadke, "Real time instability prediction through adaptive time series coefficients," IEEE Power Engineering Society, 1999 Winter Meeting (Cat. No.99CH36233), 1999, pp. 731-736 vol.1, doi: 10.1109/PESW.1999.747547.
- [13] M. Larsson, and C. Rehtanz, "Predictive frequency stability control based on wide-area phasor measurements," IEEE Power Engineering Society Summer Meeting., 2002, pp. 233-238 vol.1, doi: 10.1109/PESS.2002.1043222.
- [14] A. Sauhats, A. Utans, J. Silinevics, G. Junghans, and D. Guzs, "Enhancing Power System Frequency with a Novel Load Shedding Method Including Monitoring of Synchronous Condensers' Power Injections," Energies, vol. 14, no. 5, p. 1490, Mar. 2021, doi: 10.3390/en14051490.
- [15] U. Rudez, and R. Mihalic, "WAMS-Based Underfrequency Load Shedding With Short-Term Frequency Prediction," in IEEE Transactions on Power Delivery, vol. 31, no. 4, pp. 1912-1920, Aug. 2016, doi: 10.1109/TPWRD.2015.2503734.
- [16] S. Pulendran, and J. E. Tate, "Energy Storage System Control for Prevention of Transient Under-Frequency Load Shedding," in IEEE Transactions on Smart Grid, vol. 8, no. 2, pp. 927-936, March 2017, doi: 10.1109/TSG.2015.2476963.
- [17] E. Farantatos, R. Huang, G. J. Cokkinides, and A. P. Meliopoulos, "A Predictive Generator Out-of-Step Protection and Transient Stability Monitoring Scheme Enabled by a Distributed Dynamic State Estimator," in IEEE Transactions on Power Delivery, vol. 31, no. 4, pp. 1826-1835, Aug. 2016, doi: 10.1109/TPWRD.2015.2512268.
- [18] A. Bose, "Smart Transmission Grid Applications and Their Supporting Infrastructure," in IEEE Transactions on Smart Grid, vol. 1, no. 1, pp. 11-19, June 2010, doi: 10.1109/TSG.2010.2044899.
- [19] G. Paramo, A. Bretas, and S. Meyn, "Research Trends and Applications of PMUs," Energies, vol. 15, no. 15, p. 5329, Jul. 2022, doi: 10.3390/en15155329.
- [20] B. Naduvathuparambil, M. C. Valenti, and A. Feliachi, "Communication delays in wide area measurement systems," Proceedings of the Thirty-Fourth Southeastern Symposium on System Theory (Cat. No.02EX540), 2002, pp. 118-122, doi: 10.1109/SSST.2002.1027017.
- [21] J. Elfring, E. Torta, and R. van de Molengraft, "Particle Filters: A Hands-On Tutorial," Sensors, vol. 21, no. 2, p. 438, Jan. 2021, doi: 10.3390/s21020438.
- [22] S. Julier, J. Uhlmann, and H. F. Durrant-Whyte, "A new method for the nonlinear transformation of means and covariances in filters and estimators," in IEEE Transactions on Automatic Control, vol. 45, no. 3, pp. 477-482, March 2000, doi: 10.1109/9.847726.
- [23] G. Paramo, and A. Bretas, "Proactive Frequency Stability Scheme: A Distributed Framework Based on Particle Filters and Synchronphasors," Energies, vol. 16, no. 11, p. 4530, Jun. 2023, doi: 10.3390/en16114530.
- [24] M. S. Arulampalam, S. Maskell, N. Gordon, and T. Clapp, "A tutorial on particle filters for online nonlinear/non-Gaussian Bayesian tracking," in IEEE Transactions on Signal Processing, vol. 50, no. 2, pp. 174-188, Feb. 2002, doi: 10.1109/78.978374.
- [25] G. Paramo, and A. Bretas, "Proactive Frequency Stability Scheme via Bayesian Filters and Synchronphasors," 2023 IEEE Kansas Power and Energy Conference (KPEC), Manhattan, KS, USA, 2023, pp. 1-6, doi: 10.1109/KPEC58008.2023.10215435.
- [26] F. Zeng, J. Zhang, G. Chen, Z. Wu, S. Huang, and Y. Liang, "Online Estimation of Power System Inertia Constant Under Normal Operating Conditions," in IEEE Access, vol. 8, pp. 101426-101436, 2020, doi: 10.1109/ACCESS.2020.2997728.
- [27] L. Yu, D. Shi, G. Xu, X. Guo, Z. Jiang, and C. Jing, "Consensus Control of Distributed Energy Resources in a Multi-Bus Microgrid for Reactive Power Sharing and Voltage Control," Energies, vol. 11, no. 10, p. 2710, Oct. 2018, doi: 10.3390/en11102710.
- [28] NERC Standards, PRC-006-SERC-02, 2017.